Water Resources Management

Investigation of Wetting Front Propagation Dynamics Using Soil Impedance Measurements: Implications for Modelling and Irrigation Scheduling.

--Manuscript Draft--

Manuscript Number:	WARM-D-13-00762R1
Full Title:	Investigation of Wetting Front Propagation Dynamics Using Soil Impedance Measurements: Implications for Modelling and Irrigation Scheduling.
Article Type:	General paper
Keywords:	soil moisture measurement, wetting front detection, soil impedance, soil modelling.
Corresponding Author:	Jose Antonio Gutierrez Gnecchi, PhD Instituto Tecnologico de Morelia Morelia, Michoacán MEXICO
Corresponding Author Secondary Information:	
Corresponding Author's Institution:	Instituto Tecnologico de Morelia
Corresponding Author's Secondary Institution:	
First Author:	Jose Antonio Gutierrez Gnecchi, PhD
First Author Secondary Information:	
Order of Authors:	Jose Antonio Gutierrez Gnecchi, PhD
	Arturo Mendez Patiño, PhD
	Fernando Landeros Paramo, MSc
	Adriana del Carmen Tellez Anguiano, PhD
	Daniel Lorias Espinoza, PhD
Order of Authors Secondary Information:	
Abstract:	The authors propose a measurement method that divides the depth of the soil sample in discrete regions to investigate soil water propagation dynamics using soil impedance measurements. Experiments were conducted on a cylindrical phantom using a clay loam soil sample (60% clay, 21% loam and 19% sand). The resulting impedance changes represent the wetting front (WF) propagation process at the different measurement depths. The measured impedance data is used to A) show graphically the wetting front propagation process, obtain B) a 1st order model, C) an ARX1821 model of the impedance change as a function of the irrigation volume applied and D) estimating changes in water content using a neural network. The results indicate that the proposed measurement technique can be used to detect and predict the movement of liquid trough the soil sample. The neural network permits inferring the water content from impedance and soil-water mixture temperature values. Changes in soil impedance in each segment, due to the water propagating downwards through the soil sample, can be used to study the dynamics of the wetting front, irrigation scheduling and model improvement from physical data.

Dear George P. Tsakiris, Ph.D.
Editor-in-Chief
Water Resources Management

Thank you for your comments regarding our submission entitled "Investigation of Wetting Front Propagation Dynamics Using Soil Impedance Measurements: Implications for Modelling and Irrigation Scheduling".

We have addressed all your recommendations and have corrected the manuscript accordingly. We are including a list of responses to each comment.

==

A) Associate editor comments.

With regards to the length of the manuscript we have edited text, figures and tables to comply with the maximum number of words allowed for publication, following reviewer 1's recommendations as well. Table 1 has been deleted since all the information was already given in the paper. Now, there are 8 figures, 4 tables and the word processing software reports 4,400 words, thus complying with the maximum number of words allowed.

Further review was carried out to include recent WARM references related to the submitted work, while maintaining the contents and required length.

B) Reviewer #1 comments.

1) "There are too many results and discussion in the 3rd part "Experimental setup", which should be much shorter and only experimental details described here, and the 3.2, 3.3 and 3.4 should be moved to part of -4 Results and discussion-".

The text sequence has been edited according to the recommendation to follow the suggested sequence. As a result the text section and subsection numbering have changed, but the contents remains as in the original text.

2) "The "ARX model" in the abstract should be given with full name".

The ARX model name was updated in the abstract section as suggested.

3) "Double check with the reference of "Xuesong, 2011", especial attention with the first name and family name, and more reviewing work should be taken".

The reference has been corrected and all corresponding callouts have also been corrected. A number of references have also been included which are related to the work and support the review with information published recently. All references have been obtained through EndNote and exported in the format shown in the "Instructions for Authors" web site section.

4) How about the cost with this new method? Any comparison discussion?

There are many factors that influence the total cost of the prototype; ranging from review, design, simulation and development times to low volume purchases and component availability, and thus an accurate value for University developments is difficult to establish. Prototype development is always more expensive than the final market price. Although an estimate can be given based on allocated funding and development hours invested, we consider that giving an accurate figure for final market value would require a thorough explanation. We also consider that giving the cost only based on electronic components used would not represent the actual value. At present, explaining the proposed data processing method has occupied all the space available for one publication. However, the reported work represents only part of the functions that can be performed. We are preparing a separate paper explaining further uses of the device presented for imaging water dynamics, where a thorough explanation about cost is included.

Nevertheless, a qualitative pricing estimate is included twice in the text so that the reader can have an idea of the cost with respect to other measurement methods.

5) "Legend should be added in figure 1".

All Figures have been edited to include labels that can be used to ease explanation both in the text and in the Figure captions.

6) "1.2 should be discussed before 1.1"

We agree with Reviewer #1. The text has been edited to deliver the information presented in section 1.1 prior to section 1.2.

7) "DAS is necessary in the title of 2, actually, the DAS never been used in the paper."

The Data Acquisition System acronym has been included in the title as indicated, and used in the text. The recommendation contributed to shorten the length of the paper to comply with the maximum length allowed.

8) "Attentions should be taken with the lines of tables."

All tables have been re-edited to adjust the tabulation settings to improve reading.

==

On behalf of the authors, thank you for your help in processing our paper. Please contact me if you require any further information.

Best Regards

José Antonio Gutiérrez Gnecchi
Corresponding Author.

Investigation of Wetting Front Propagation Dynamics Using Soil Impedance Measurements: Implications for Modelling and Irrigation Scheduling.

Jose Antonio Gutierrez Gnecchi[a1] , Arturo Mendez Patiño[a], Fernando Landeros Paramo[a], Adriana del Carmen Tellez Anguiano[a] and Daniel Lorias Espinoza[b].

[a]Instituto Tecnológico de Morelia, Departamento de Ingeniería Electrónica, Avenida Tecnologico 1500, Col. Lomas de Santiaguito, C. P. 58120, Morelia, Michoacan, Mexico. Telephone: (52) 4433121570 ext. 270. Email: biodsprocessing@aol.com

[b]CINVESTAV/IPN, Av. Instituto Politécnico Nacional 2508, Col. San Pedro Zacatenco, C.P. 07360 México, D.F., México. Telephone: (52) 5557473800. Email: dlorias@cinvestav.mx

Abstract.

The authors propose a measurement method that divides the depth of the soil sample in discrete regions to investigate soil water propagation dynamics using soil impedance measurements. Experiments were conducted on a cylindrical phantom using a clay loam soil sample (60% clay, 21% loam and 19% sand). The resulting impedance changes represent the wetting front (WF) propagation process at the different measurement depths. The measured impedance data is used to A) show graphically the wetting front propagation process, obtain B) a 1st order model, C) an ARX1821 model of the impedance change as a function of the irrigation volume applied and D) estimating changes in water content using a neural network. The results indicate that the proposed measurement technique can be used to detect and predict the movement of liquid trough the soil sample. The neural network permits inferring the water content from impedance and soil-water mixture temperature values. Changes in soil impedance in each segment, due to the water propagating downwards through the soil sample, can be used to study the dynamics of the wetting front, irrigation scheduling and model improvement from physical data.

Keywords: soil moisture measurement, wetting front detection, soil impedance, soil modelling.

1. Introduction

Accurate knowledge of water propagation dynamics though soil is of great importance for agricultural and geological studies. Amongst the processes that benefit from modelled and in-situ data are prediction of

[1] Corresponding author

groundwater and aquifer recharge (Patterson and Bekele 2011), waste water and contaminant migration assessment (Baram et al. 2012) and water resources management. Thus, wetting front modelling efforts are continuously reported, for instance, for predicting potential recharge (Ali et al. 2013), overland flow (Pantelakis et al. 2011) and for studying soil infiltration properties as a function of soil roughness (Zhao et al. 2013).

In particular for irrigation scheduling, hydraulic conductivity and wetting front propagation properties play an important role towards achieving true precision agriculture. Thus, proposals of new and applied models of soil hydraulic properties based on theoretical (Dorofki et al. 2014) and empirical (Elmaloglou and Malamos 2007) data are commonly reported. However, soil hydraulic conductivity properties vary continuously as a function of many factors ranging from soil preparation, tillage treatment and soil content (chemical and mineral) up to weather conditions. Therefore methods for laboratory (Argyrokastritis et al. 2009) and in-situ measurements for improving modelling are commonly reported.

1.1 Wetting Front (WF) propagation through soil

Upon applying water to the soil, water infiltrates forming a wetting front, defined as the frontier between the region where water has infiltrated and the rest of the soil (Figure 1).

Fig. 1. Wetting front visual observation in an experimental rhizotron/lysimeter (Gutierrez-Gnecchi et al. 2011 © [2011] IEEE). A) First, B) second and C) third experiment

As water propagates, the colour of the soil sample darkens, allowing visual identification of the wetting front frontier in the test container. Knowledge of the depth the wetting front reaches before vanishing for a given volume of water, can be used for managing irrigation. Therefore simple mechanical devices (Strizaker 2003) such as the FullStop Wetting Front Detector (FS WFD) have been widely adopted by farmers. The FS WFD is a funnel buried in the soil that allows detecting when the wetting front has reached a given depth, and collection of the corresponding solution. The FullStop WFD gives an indication of the WF propagating speed along the depth of the soil as a whole. Since the soil hydraulic properties change dynamically, the WF propagation properties change even for the same test conditions. Figure 1 shows the WF propagation speed for three experiments using the same amount of water; It can be observed that the WF depth varies from one experiment to the other.

1.2 Soil moisture measurement techniques

There are three main methods for soil moisture measurement: gravimetric, nucleonic and electromagnetic techniques (Kelleners 2005). The advances in electronics, instrumentation and digital signal processing hardware over the last two decades have benefited the increasing popularity of electromagnetic methods since they allow fast, non-destructive and automated soil moisture measurements. Amongst the most common electromagnetic techniques are TDR (Time Domain Reflectometry) (Topp 1980; Mao et al. 2011), capacitance (Kinzli et al. 2012), and impedance (Robinson et al. 2003) measurements. Other electromagnetic techniques such as Ground Penetrating Radar (GPR) (Strobachk et al. 2012), Electrical Resistance Tomography (Beff 2012) and multimodal measurement systems (Gil-Rodriguez et al. 2013; Gutierrez-Gnecchi et al. 2012), are also being reported continuously.

1.3 Measurement of wetting front (WF) propagation dynamics

Following the introduction of the FS WFD, a number of automated devices have been proposed to try to fill the gap between visual observations and controlling the irrigation process (Drury 2002; Gutierrez-Gnecchi et al. 2011); although they can be used for irrigation control, they do not yield detailed WF dynamics information along the entire depth. Some of the attempts to measure the dynamics of WF involve the use of a number of TDR probes inserted in a test vessel at different depths (Mao et al. 2011). However, the widespread use of TDR sensor technology is often impeded by cost and lack of local technical support. Similarly, the use of Electrical Impedance Tomography (EIT) can produce an image to reveal WFD dynamics. Although complex measurement systems work well at laboratory level, are not always suitable for wide use in the field. In addition, despite the variety of sensing methods reported, measurement errors (Hook and Livingston, 1996) and uncertainties (Walker et al. 2006) require empirical calibration for specific sites (e.g. Herkelrath et al. 1991; Quinones et al. 2003). Therefore, there are incentives to continue developing tools and methods that can provide in-situ information with minimal recalibration requirements. Here the authors propose that there may be a middle ground between complex electrical impedance imaging techniques and simple mechanical devices to measure WF dynamics. A set of electrodes separated equidistantly along the soil depth, together with a dedicated instrumentation, can be used to measure the changes in soil impedance as water propagates through the samples.

2. Data Acquisition System (DAS) design

Figure 2 shows the schematic diagram of the DAS equipment designed for WF measurements.

Fig. 2. A) Sensor array. B) Block diagram of the data acquisition system: 1) 1.5 MHz sinewave generator, 2) second order bandpass filter, 3) programmable gain voltage controlled current source (VCCS), 4) analogue multiplexer array, 5) electrode array connection, 6) instrumentation amplifier, 7) 90o phase shift circuit, 8) Root-Mean-Square (RMS) converter, 9) microcontroller unit. 10) VCCS gain control lines, 11) multiplexer selection lines, 12) serial interface, 13) display interface, 14) keyboard input, 15) Secure Digital interface and 16) JTAG in-system programming interface.

The sensor array comprises eight 1-inch electrodes attached to a 1-inch diameter CPVC pipe. The electrodes are separated 7 cm along the pipe length. The DAS uses a 1.5 MHz, 1Vpp sinewave as excitation signal. A second order bandpass filter is used to filter out noise and unwanted harmonics. Although soil impedance measurements reported use excitation signals in excess of 50 MHz, the maximum operating frequency is constrained by the analogue electronics bandwidth, to maintain a cost-effective design. The excitation signal is fed to a programmable-gain voltage controlled current source (VCCS) circuit. Five different excitation signal amplitudes can be selected: 2.21 mA, 0.212mA, 450μA, 45 μA and 21.21μA. The current excitation signal is conveyed towards the electrodes through an array of two analogue multiplexer circuits. When the current signal is applied to the soil sample, a voltage develops across the electrode pair. Since the current signal is known and the corresponding voltage is measured, it is possible to calculate the soil impedance. An RMS-to-DC converter provides a direct current representation of the measured voltage. The microcontroller then calculates the corresponding soil impedance.

The prototype includes a serial communication interface to transfer the data to a host PC, a liquid crystal display (20 X 3), keyboard and adapter for an SD memory card. Without data compression, a 1GB SD card allows registering up to 250,000 1-hour experiments, sampling at 60 second intervals. The prototype also includes a JTAG interface so that further signal processing algorithms can be included without changing the hardware.

3. Experimental Setup

In order to test the DAS equipment (Figure 3A), the sensor array (Figure 3B) was inserted into a 3-inch diameter CPVC pipe, filled with clay loam soil (60% clay, 21% loam and 19% sand) (Figure 3C). The initial water content was measured using a TDR sensor (Campbell Scientific CS616) to be 12%. Irrigation was applied at a rate of 1.5 l h-1 into a 2.43 l container volume. 1.15 litres of water were added over a period of 45 minutes at a rate of 1 sample per minute. Table 1 shows the chemical properties of the water used for the experiment.

Fig. 3. A) Data acquisition system, B) electrode array and C) experimental vessel

Table 1. Chemical properties of the water used for the experiment.

The measurement process starts by selecting the sampling rate, which can be adjusted in steps of 1 minute up to 15 minutes. The DAS can also be adjusted to measure in differential sequence or linear-array electrical impedance tomography (EIT) sequence. In differential sequence the equipment selects pairs of consecutive electrodes (i. e. electrodes 1-2, electrodes 2-3 and so on) to determine the changes in resistivity between electrodes due to the irrigation process; thus the sensing length is divided in 7 measurement levels for 8 electrodes. In linear-array EIT mode, the electrodes are selected in pairs in all different combinations yielding 28 measurements for 8 electrodes. This work discusses only the results from measuring in differential mode, using the impedance modulus.

4. Experimental Results

4.1 One-dimensional wetting front detection in Clay-loam soil

Figure 4A shows the results of the test trial. The small enclosure intends to constrain the water propagation downwards to resemble a one-dimensional wetting front movement as close as possible.

Fig. 4. A) Test results. B) Graphical example of WF calculation arrival at location between electrode 1 and 2. C) Filtered Slope (FS) calculations to determine WF arrival at the different electrode pair locations.

As water progresses through the sample, the soil impedance between electrodes decreases indicating the arrival of the wetting front. Since the sample time is fixed, assigning a time stamp for the arrival of the wetting front at the different depths can be achieved by calculating the filtered slope, S_F, of the soil impedance measurement data set (1):

$$S_F(k) = \frac{R(k+m-1)-R(k)}{m} \quad k = 1..n-m \tag{1}$$

where R(k) is k^{th} soil impedance measurement at the fixed excitation frequency, n is the total number of samples per data set and m is the number of samples around the slope calculation. The time corresponding to the minimum value of $S_F(k)$

$$WFD(k) = min\{S_F(k)\} \tag{2}$$

is chosen to indicate the arrival of the wetting front (WFD: Wetting Front Detection) at the corresponding depth. Figure 4B shows the WFD calculation results using three data measurements (m=3), for detecting the arrival of the wetting front at location 1: between electrode pair 1-2.

The minimum value of the slope, $S_F(k)$, occurs at 11:29:36; that is 9 minutes after the test trial was initiated. Since the electrode pair is located 7 cm below the soil surface, the wetting front propagation rate is 46 cm h^{-1}. The value is the result of a small containment volume, low initial soil water content, and a considerable large amount of water used in the test trial. Nevertheless, the results show that the procedure can yield the propagation velocity using simple on-line signal processing algorithms. Calculation of the wetting front arrival at the different electrode locations is shown in Figure 4C.

Table 2 shows a summary of the WFD propagation speed results trial.

Table 2. WFD propagation speed measurements

The results show that the propagation speed varies along the length of the soil sample. Dividing the measured depth in discrete steps can give a more accurate representation of the layered propagation speed for a given soil sample.

4.2 Modelling of wetting front response

Complex mathematical procedures have been proposed to try to determine the dynamics of water propagation through soil down to the pore size (Guber 2009). However, water propagating through soil is a slow process; in addition, for irrigation scheduling the control systems involved are commonly on-off timer operated systems. Therefore a simple approach for modelling may be derived from direct multilevel impedance measurements. Consider the first order model in the frequency domain (e. g. **s** domain) given by (3):

$$R(s) = \frac{K_P e^{-sT_D}}{s\tau + 1} \tag{3}$$

Where R(s) is the process transfer function (i.e. soil resistivity), **s** is a complex number, K_P is the system gain (Ω s l^{-1}), τ is the time constant and T_D is the time delay. Considering further that the system response corresponds to a constant volume of water added (step input), a model can be derived from direct measurements. The step input has a magnitude H_0= 4.16666e-04 l s-1 (1.5 l h^{-1}). Calculating the initial conditions and system gain involves obtaining the minimum and maximum impedance values measured. The initial condition, R(0), is the maximum impedance value. Parameter K_P will be the difference between the minimum and maximum resistivity values, divided by the magnitude of the step function.

$$K_P = \frac{min\{R(k)\} - max\{R(k)\}}{H_0} \tag{4}$$

The time constant, τ, is assigned for each measurement pair representation to be the difference between the wetting front detection times between pairs of electrodes. Starting from cero for the first pair of electrodes, each time delay value is the cumulative time between previous wetting front detection times. Table 3 shows the parameters used for modelling soil resistance changes for each measurement site.

Table 3. 1st order model parameters for each electrode pair site derived from direct measurements

The discrete solution of (3) for a step input is then

$$R(k) = R(0) + H_0\left(K_P\left(1 - e^{\frac{-kT}{\tau}}\right)\gamma(kT - T_D)\right) \tag{5}$$

where T is the sample time and $\gamma(kT-T_D)$ represents the delay. Figure 5 shows the results of approximating the soil resistivity change compared to impedance measurements. Although the model fits the estimation to the measurement data at the WF detection point, is a coarse approximation to the measurement data. However, for irrigation scheduling purposes it may suffice to provide a prediction of the depth reached by the wetting front for a given volume of water added.

Fig. 5. First order plus delay approximation for modelling soil water wetting front propagation dynamics.

4.3 ARX modelling

A method, commonly used for modelling and system identification from direct measurements consists of obtaining a discrete dynamic autoregressive (with external input) polynomial representation of the response (ARX). The ARX model structure can be implemented from real measurements to give an accurate representation of the water propagation process based on soil impedance measurements. A text-book definition of the dynamic ARX model structure is given by (6)

$$A(q)y(t) = B(q)y(t - nk) + e(t) \quad (6)$$

where A(q) defines the number of poles, B(q) is the number of zeroes, nk is the delay and e(t) is the noise term. One of the advantages of implementing (6) is that requires relatively small computation resources and can be implemented as part of the microcontroller programming. Perhaps the most difficult part consists on choosing the appropriate number of model parameters, for a given data set and the morphology of the resulting graph. An off-line test showed that 18 poles, 2 zeroes can yield more than 95% fit approximation. Thus an ARX1821 model was implemented on the microcontroller. Table 4 shows the resulting ARX1821 model parameter for each electrode pair measurement site, for the case presented in particular.

Table 4. Discrete Time ARX model: A(z)y(t)=B(z)u(t)+C(z)e(t), sampling time, T=60 s. Step input= 4.1666666 l s^{-1}

Figure 6 shows the result of approximating the resistance changes using the ARX1821 model.

Fig. 6. ARX1821 approximation of the impedance changes due to a water step input of 1.5 l h^{-1}.

The ARX modelling approach yields a closer representation of the wetting front propagation through the soil sample.

4.4 Deriving the water content in the soil sample from resistance measurements

The analysis procedures shown in sections 4.2 and 4.3 use impedance change measurements to detect and model the propagation dynamics of the wetting front which may be suitable for irrigation scheduling. However the impedance measurements do not yield information about the water content in the soil sample. In addition, the temperature of the soil-water mixture greatly influences impedance measurements.

In order to obtain water content information from electrical measurements, the impedance of 20 soil samples was obtained for different water contents (Figure 7A) ranging from 5% up to 60% (by weight) at two different temperatures (25 ^{o}C and 30 ^{o}C) (Figure 7B).

Fig. 7. A) Schematic diagram of the experimental setup for measuring soil impedance as a function of the water content and mixture temperature. B) Impedance values measured as a function of the water content for two different temperatures.

The impedance values vary depending on the temperature of the mixture. To compensate for temperature variations, and infer water content from impedance measurements, the results were used to train a two-layer neural network commonly used for function approximation. The neural network (Figure 8A) can yield considerable good results for approximating a considerable complex signals.

Fig. 8. A) Two later backpropagation neural network used for estimating water content from impedance measurements. B) Neural network estimation of the soil water content from resistivity measurements at the different electrode pair sites

Moreover, the neural network can be trained and implemented for on-line operation. The first layer consists of 3-atansigmod neurons with transfer function given by (7):

$$\mathrm{atan}(n) = \frac{2}{(1+e^{-2n})-1} \qquad (7)$$

The second layer is a single linear neuron with transfer function (Figure 7A). The network was trained using the backpropagation method with momentum (8):

$$\Delta W(i,j) = mc\,\Delta W(i,j) + (1-mc)lr\,D(i)P(j) \qquad (8)$$

where ΔW(i,j) represents the weights adjustment, mc is the momentum constant (mc=0.95), D(i) are derivatives of errors (delta vectors), an lr=0.1 is the learning rate. 40 Temperature and 40 impedance values were presented to the network during 100 to 200 epochs until reaching a Sum of Squares Error (SSE) of 0.1. The target vector contained the water content data corresponding to each soil sample tested. The resistivity values were scaled down to the range of 0 to 2.5 (2.5 for 117000 Ohms and 0 for 0 Ohms) and the humidity content scale used was from 0 to 1 (1 for 100% and 0 for 0% water content).

Figure 8B shows the estimated percentage of water content for each test site. At the end of the experiment, five 100g samples were obtained from the container, corresponding to the first five electrode measurement sites. From the gravimetric method the average water content was 47.8%, in agreement with the estimated measurements using the neural network.

5. Discussion

Measuring soil resistivity at different depths allows obtaining a more detailed representation of the WF dynamics, compared to a single depth or volumetric measurements. In section 4.1 it was shown that the propagation speed varies along the depth even for a uniform soil sample. Thus calculating the arrival of the wetting front at different depths can be implemented easily from direct resistivity measurements, to adjust for changes in hydraulic conductivity properties. Impedance values can also be approximated for irrigation scheduling; a simple 1st order model, coarse approximation, can be on-line obtained and adjusted depending on historical data. A more detailed description can be obtained from ARX modelling as well with a fit percentage better that 99% in 5 out six cases based on the same procedure. Since the temperature of the soil-water mixture has a large effect on resistivity values, the water content can also be back-calculated from impedance measurements given that sufficient data is available for a given soil sample.

The equipment developed for this application is a versatile device, intended for in-situ operation that permits obtaining a vast amount of dynamical information from resistivity measurements. The different current settings included are intended to accommodate different soils. The electrode array is simple, easily reproducible, and compact. At present, simple signal processing algorithms are included; however the in-system programming feature permits including further processing features. Overall is a considerable simple device that can yield detailed information about the dynamics of wetting front propagation for further modelling the WF process.

6. Conclusions

Using discrete resistivity measurements along the depth of a soil sample can be used to provide a detailed description of the dynamics of wetting front propagation which could be used to improve current modelling procedures. The dedicated data acquisition system allows registering a large number of measurements and/or test data. A simple filtered slope calculation of the changes in resistivity quantitatively describes the arrival of the wetting front at different depths. The resistivity values can then be used for on-line calculation of simple models which in turn can be used to predict the movement of liquid through the soil sample. Furthermore, particular models can be updated based on historical data and related to soil usage. Additional important information can be derived from impedance data, such as the water content. Although it is required that the impedance data for given water content is known, the equipment can be updated for the new settings using the in-system programming feature. The resulting equipment and method presented here are a, cost-effective, versatile alternative to accurate but pricey commercial equipment and represent a middle ground between simple mechanical devices and complex imaging instrumentation systems. For irrigation scheduling, the results indicate that it may be possible to control the exact amount of water required to reduce liquid waste and improve the conditions, for instance, for horticultural crops that often are over-irrigated.

7. Acknowledgments

The authors acknowledge the financial support from SEP/ DGEST and CONACYT to carry out this work.

8. References

Ali S, Ghosh NC, Singh R, Sethy BK (2013) Generalized Explicit Models for Estimation of Wetting Front Length and Potential Recharge. Water Resources Management 27(7): 2429-2445.

Argyrokastritis I, Kargas G, et al. (2009) Simulation of Soil Moisture Profiles Using K(h) from Coupling Experimental Retention Curves and One-Step Outflow Data. Water Resources Management 23(15): 3255-3266.

Baram S, Kurtzman D, Dahan O (2012) Water Percolation Through a Clayey. J Hydrol 424–425:165–171.

Beff L, Gunther T, Vandoorne B, Couvreur V, Javaux M (2012) Soil Water Content Monitoring in a Maize Field Using ERT. Hydrol Earth Syst Sci Discuss 9, 8535–8578.

Deinert, MR, Parlange, J-Y, Steenhuis T, Throop J, Ünlü K, Cady KB (2004) Measurement of fluid contents and wetting front profiles by real-time neutron radiography. J of Hydrol 290, 192–201.

Dorofki M, Elshafie A., et al. (2014) A GIS-ANN-Based Approach for Enhancing the Effect of Slope in the Modified Green-Ampt Model. Water Resources Management 28(2): 391-406.

Drury C. 2002. The FullStop Controller: A device for Controlling Irrigation, CSIRO Land and Water Canberra, Technical Report6/02, Feb. 2002.

Elmaloglou ST, Malamos N (2007) Estimation of Width and Depth of the Wetted Soil Volume Under a Surface Emitter, Considering Root Water-Uptake and Evaporation. Water Resources Management 21(8): 1325-1340.

Gil-Rodríguez M, Rodríguez-Sinobas L, Benítez-Buelga J., Sánchez-Calvo R (2013) Application of Active Heat Pulse Method with Fiber Optic Temperature Sensing for Estimation of Wetting Bulbs and Water Distribution in Drip Emitters: Soil and Irrigation Sustainability Practices (special issue). Agr Water Manage 120, 72–78.

Guber AK, Pachepsky YA, van Genuchten MTh, Simunek J, Jacques D, Nemes A, Nicholson TJ, and Cady RE (2009) Multimodel Simulation of Water Flow in a Field Soil Using Pedotransfer Functions. Vadose Zone J. 8 (1), 1-10.

Gutierrez-Gnecchi JA, Landeros-Paramo F, Tellez-Anguiano A, Mendez-Patino A, Lobit P (2011) Automated Wetting Front Detector. In: Proceedings: IEEE Electronics, Robotics and Automotive Mechanics Conference (CERMA), 15-18 November, Cuernavaca, Morelos, Mexico, 320-324.

Gutiérrez Gnecchi JA, Gómez-Tagle Chávez A, Chavez Campos GM, Olivares Peregrino VH, Marroquin Pineda E (2012) Soil Water Infiltration Measurements Using Electrical Impedance Tomography. Chem Eng J 191:13–21.

Herkelrath WN, Hamburg SP, and Murphy F (1991) Automatic, real-time monitoring of soil moisture in a remote field area with time domain reflectometry. Water Resour Res 27(5):857-864.

Hook WR, Livingston NJ (1996). Error in Converting Time Domain Reflectometry Measurements of Propagation Velocity to Estimates of Soil Water Content. Soil Sci Soc Am J 16 (1):35-41.

Kelleners TJ, Robinson DA, Shouse PJ, Ayars JE, Skaggs TH (2005) Frequency Dependence of the Complex Permittivity and its Impact on Dielectric Sensor Calibration in Soils. Soil Sci Soc Am J 69:67-76.

Kinzli K, Manana N, Oad R (2012) Comparison of Laboratory and Field Calibration of a Soil-Moisture Capacitance Probe for Various Soils. J Irrig Drain Eng 138(4):310–321.

Mao X, Ling S, Zheng X, Kong L (2011) Moisture migration test investigation about subgrade filled with different soil. In: Proceedings 2011 International Conference on Transportation, Mechanical, and Electrical Engineering (TMEE), December 16-18, Changchun, China, 2082 – 2085.

Pantelakis D, Zissis T, Anastasiadou-Partheniou E, Baltas E (2012) Numerical Models for the Simulation of Overland Flow in Fields Within Surface Irrigation Systems. Water Resources Management 26(5): 1217-1229.

Patterson BM, Bekele EB (2011) A Novel Technique for Estimating Wetting Front Migration Rates Through the Vadose Zone Based on Changes in Groundwater Velocity. J Hydrol 409:538-544.

Quinones H, Ruelle P, Nemeth I (2003) Comparison of Three Calibration Procedures for TDR Soil Moisture Sensors. Irrig and Drain 52(3):203-217.

Robinson DA, Jones SB, Wraith JM, Or D, Friedman SP (2003). A Review of Advances in Dielectric and Electrical Conductivity Measurement in Soils Using Time Domain Reflectometry. Vadose Zone J 2 (4):444-475.

Strizaker R (2003) When to Turn the Water Off: Scheduling Micro-irrigation With a Wetting Front Detector. Irrig Sci 22:177–185.

Strobachk E, Harris BD, Dupis JC, Kepic A W, Martin M (2012). Time-lapse Borehole Radar Measurements in a Sandy Groundwater System During a Winter Recharge Cycle. In: Proceedings: 14th International Conference on Ground Penetrating Radar (GPR), 4-8 June, 2012, Shanghai, China, 689-694.

Topp GC, Davis JL, Annan AP (1980). Electromagnetic Determination of Soil Water Content: Measurements in Coaxial Transmission Lines. Water Resour Res 16(3):574-582.

Walker C, Lin HS, Fritton DD (2006). Is the Tension Beneath a Tension Infiltrometer What We Think It Is? Vadose Zone J 5:860-866.

Zhao L, Wang L, Liang X, Wang J, Faqui Wu (2013) Soil Surface Roughness Effects on Infiltration Process of a Cultivated Slopes on the Loess Plateau of China. Water Resources Management 27(14): 4759-4771.

Figure 1_Rizhotron_edited
Click here to download high resolution image

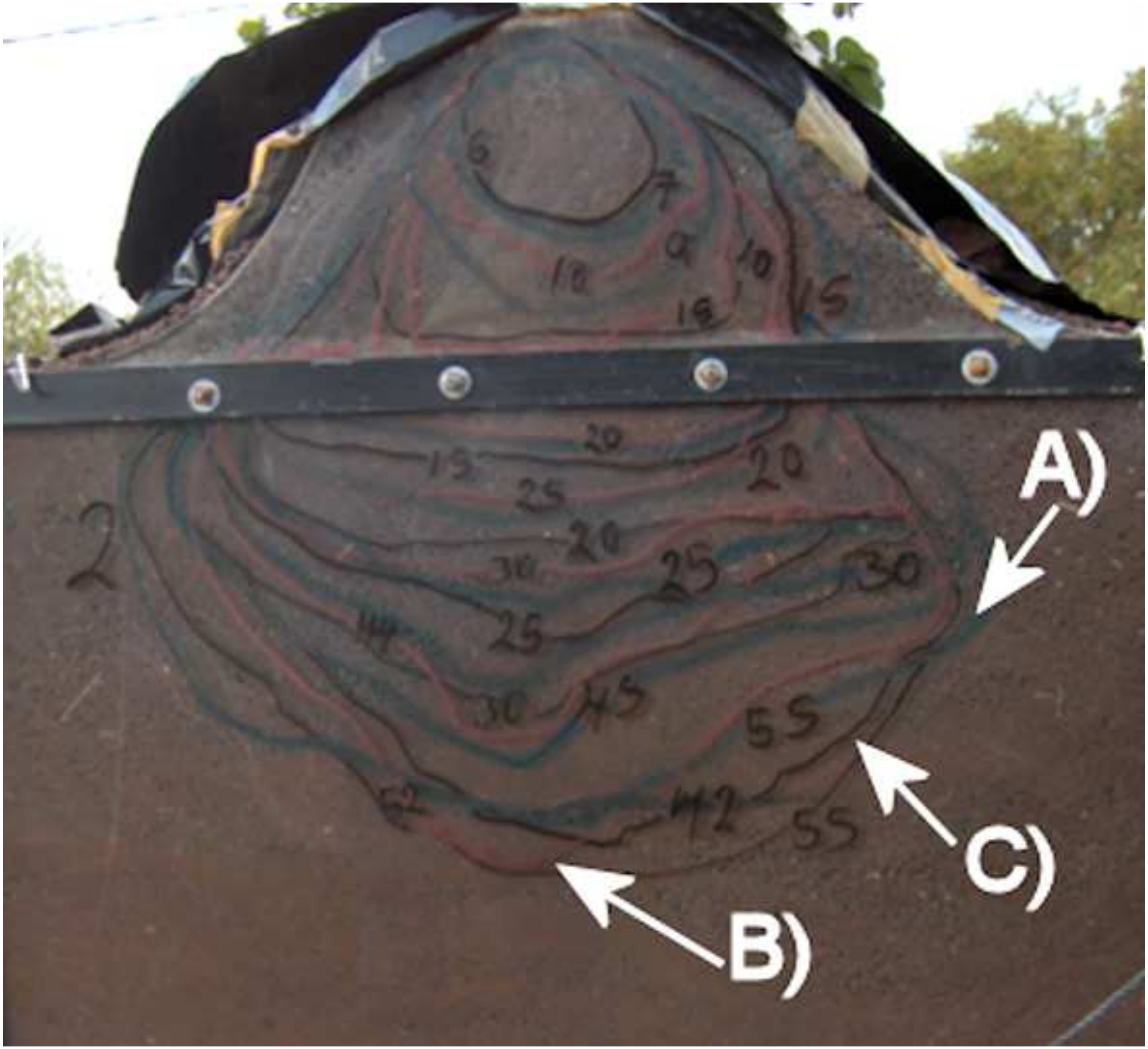

Figure 2_DAS_Schematic_block_diagram

Click here to download high resolution image

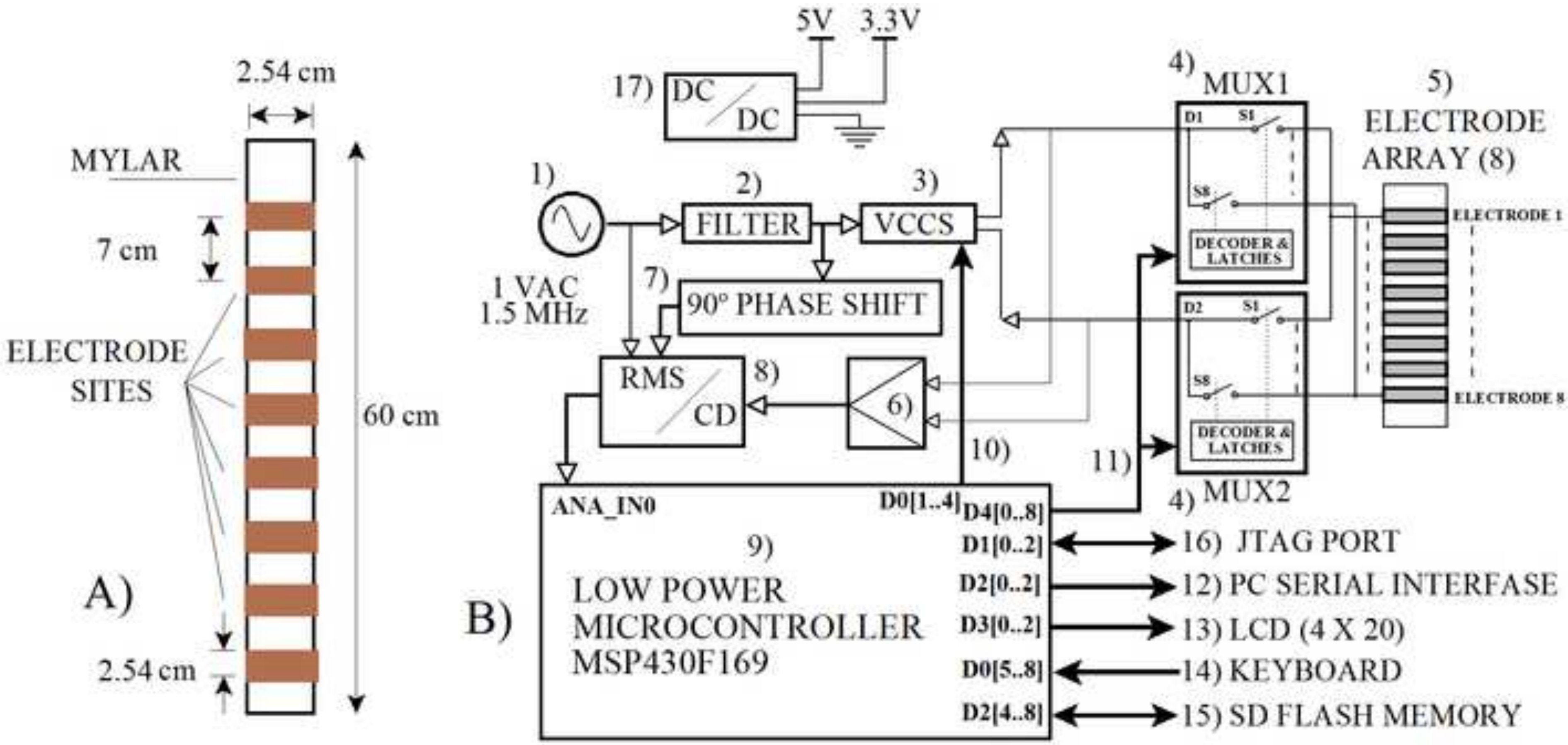

Figure 3_Electrode_system

Click here to download high resolution image

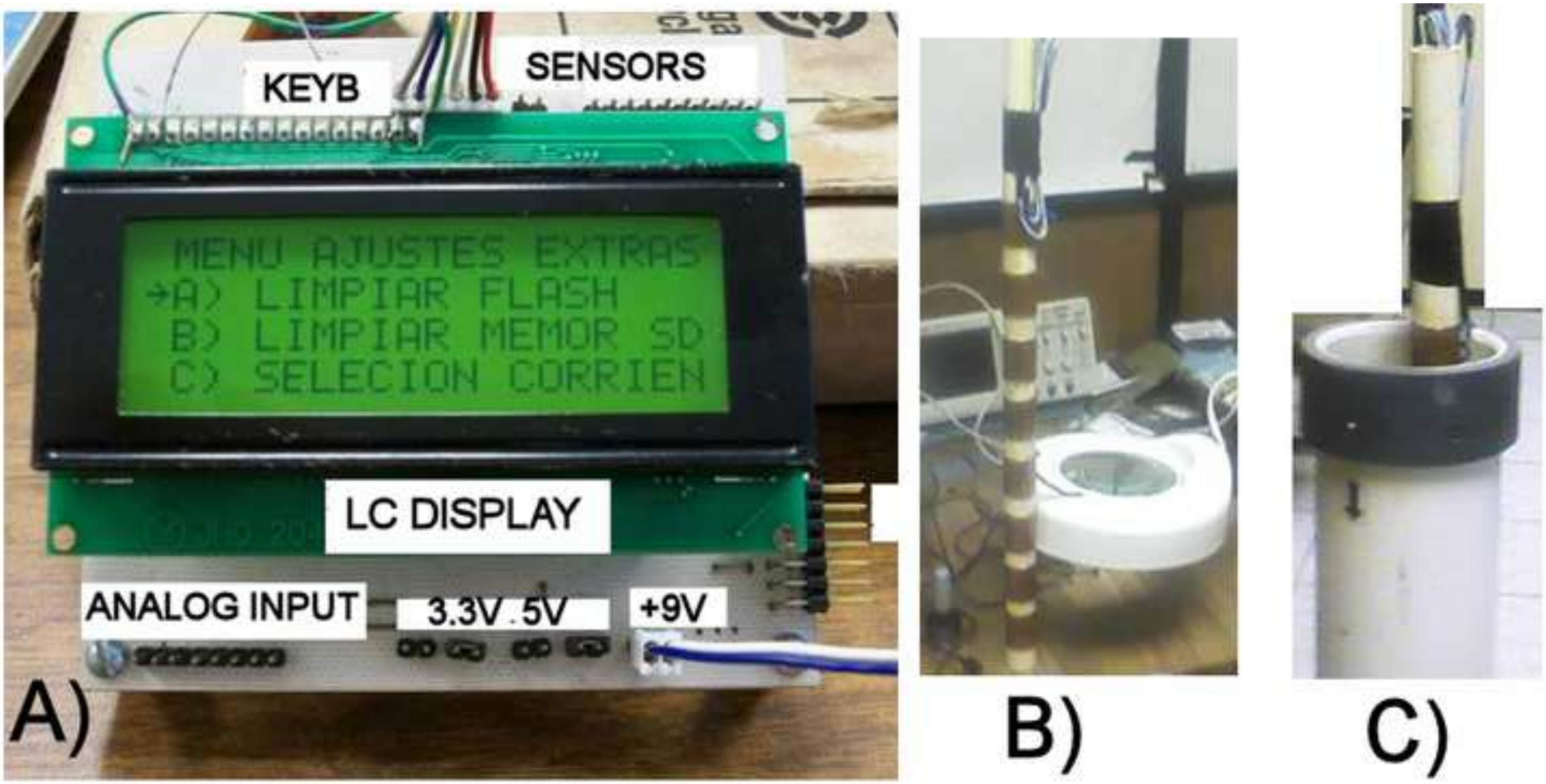

Figure 4_Measurement_and_calculations
Click here to download high resolution image

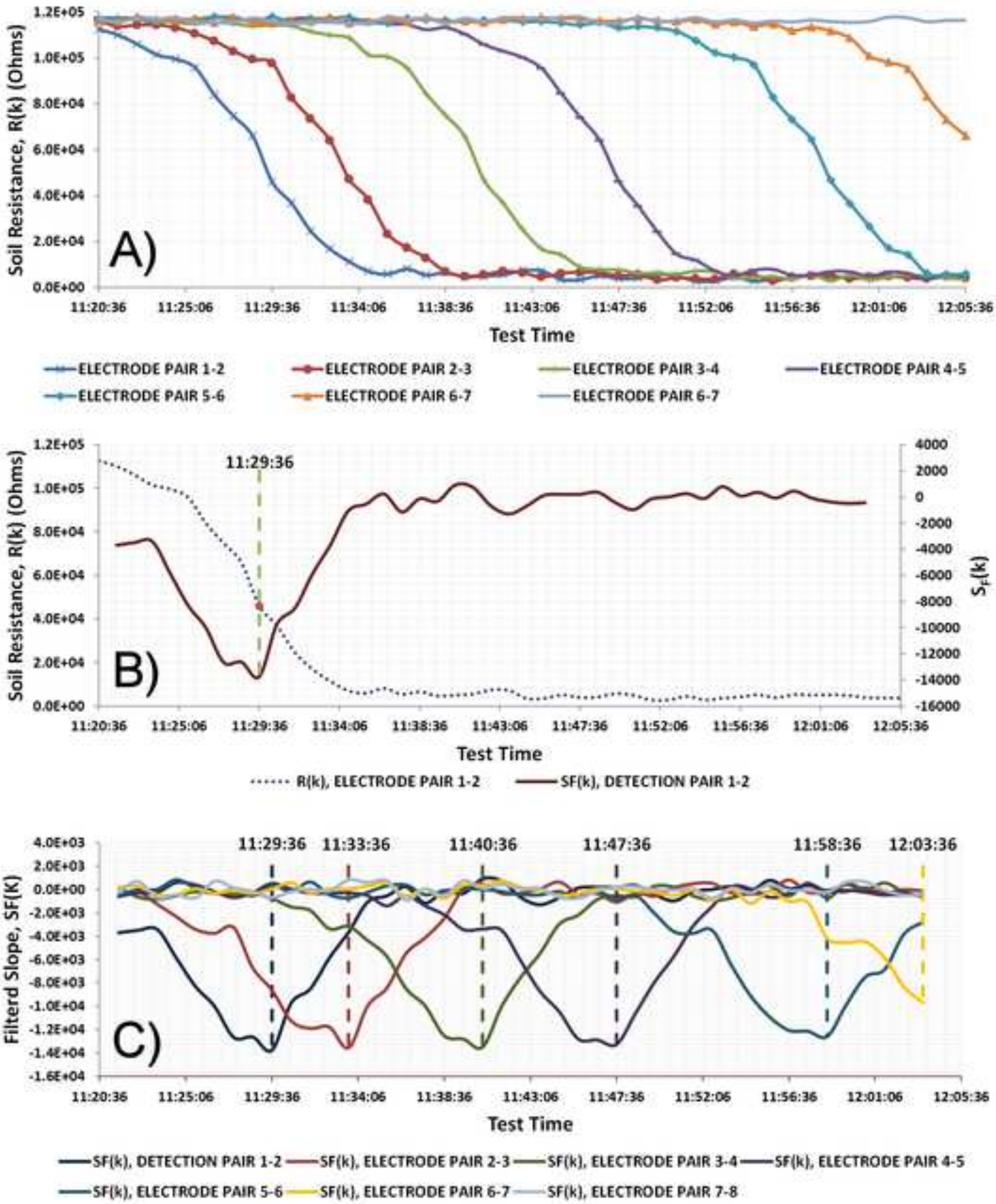

Figure 5_1st_order_model
Click here to download high resolution image

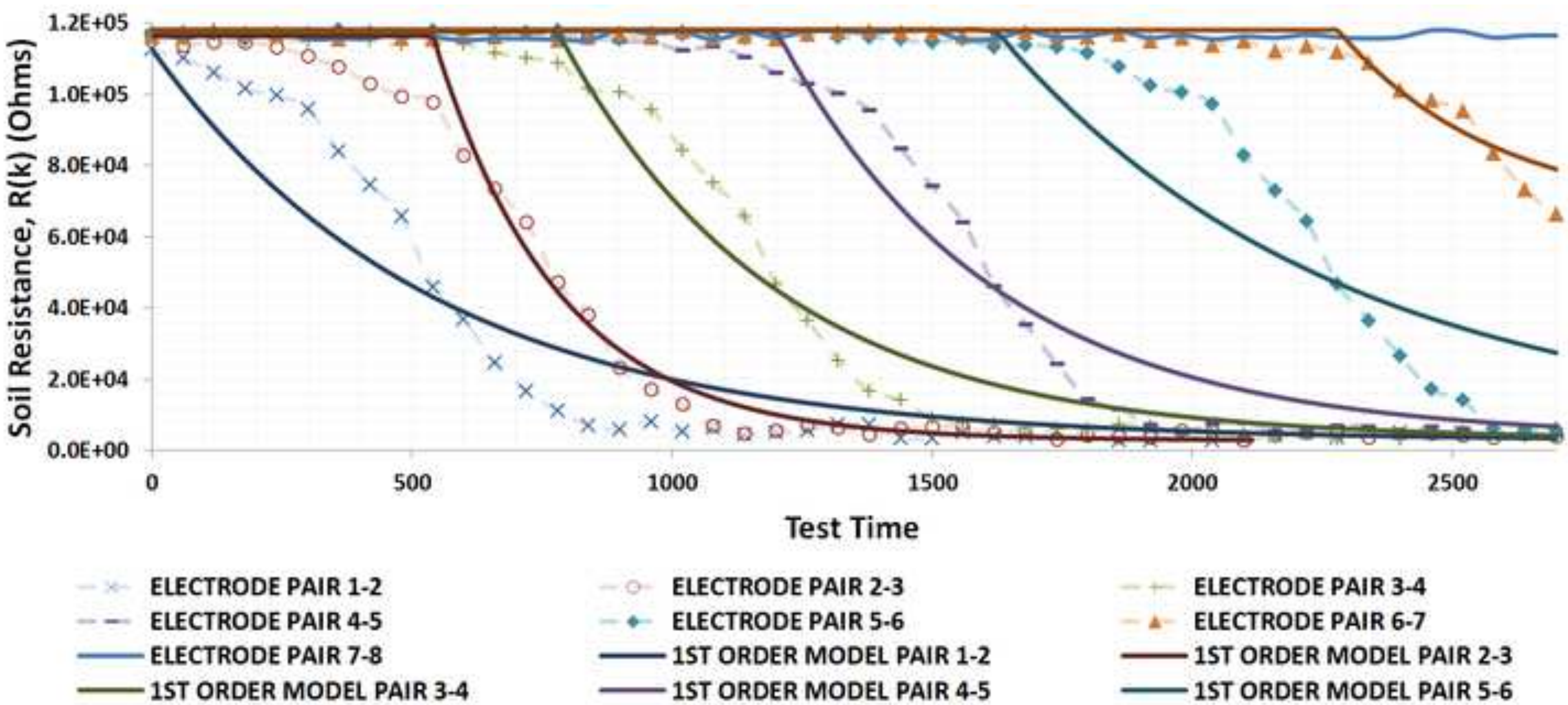

Figure 6_ARX1821_model
Click here to download high resolution image

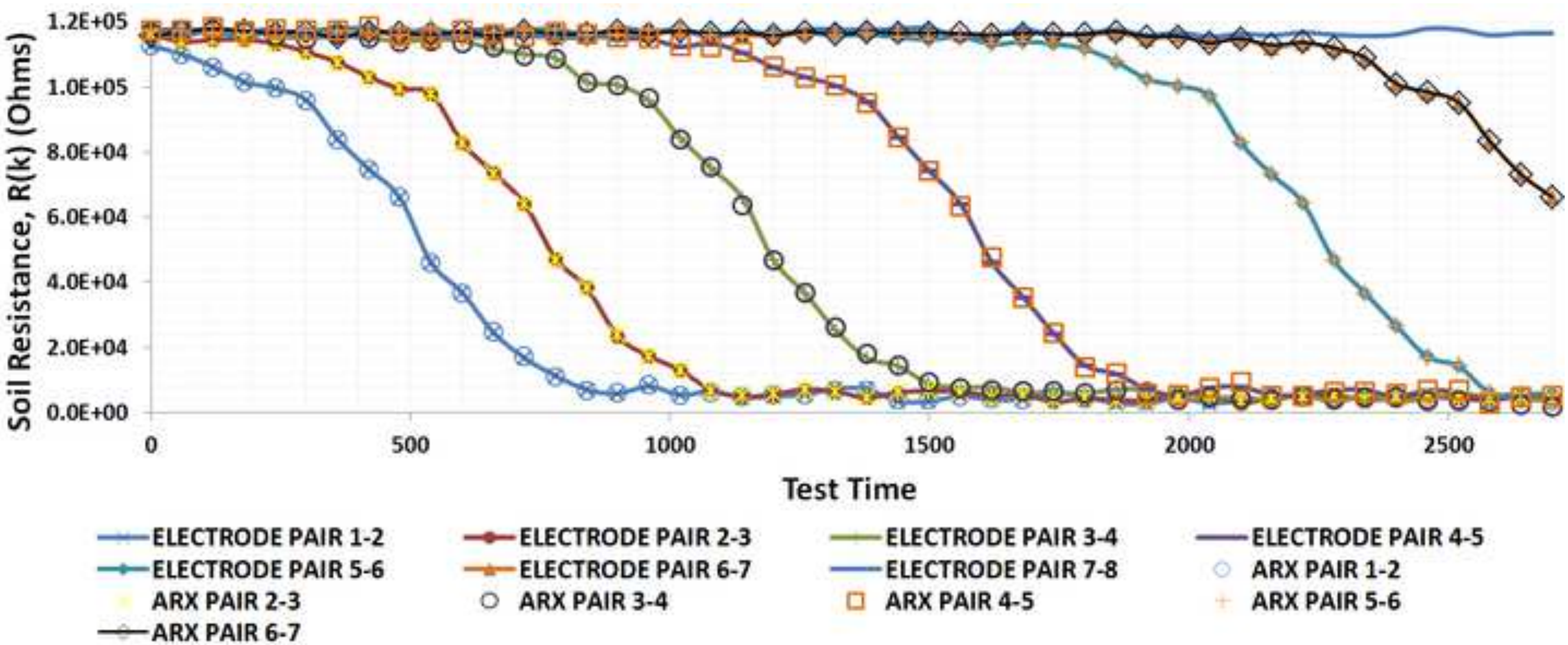

Figure 7_Temperature_adj
Click here to download high resolution image

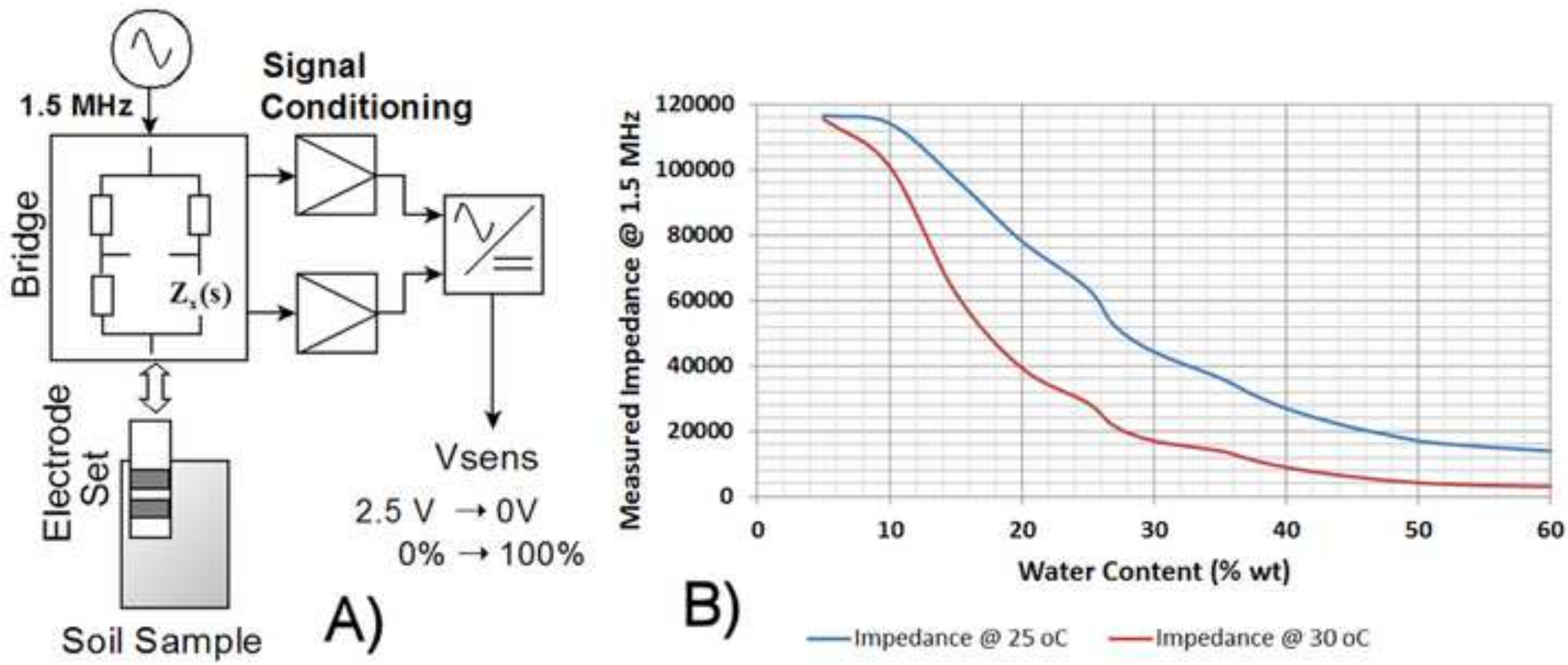

Figure 8_ANN_results
Click here to download high resolution image

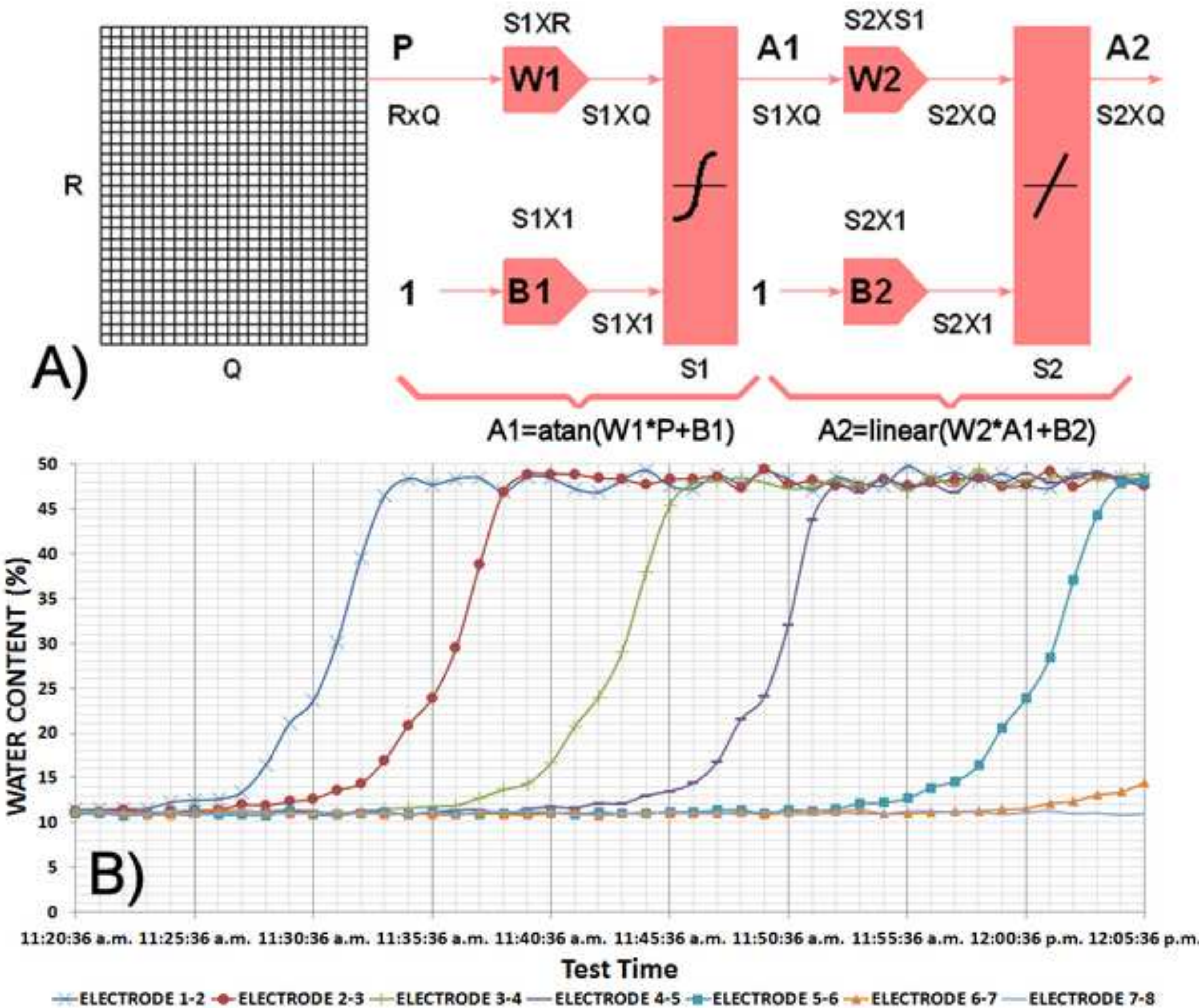

Table 1. Chemical properties of the water used for the experiment.

pH	Conductivity		Anion (mg/l)				Cation (mg/l)		
	(mS/cm)	CO32-	HC03-	Cl2-	SO42-	Na+	K+	Ca+	Mg+
6.35	210.3	0	67	47.96	19.2	8.4	2.81	42.1	39.5

Table 2. WFD propagation speed measurements

Electrode pair measurement site	1-2	2-3	3-4	4-5	5-6	6-7	7-8
Detection time (min)	9	13	20	27	38	43	-
WFD speed (cm min^{-1})	0.777	0.875	1.05	1.03	0.921	0.976	-

Table 3. 1st order model parameters for each electrode pair site derived from direct measurements

Electrode pair	max{R(k)}, R(0)	min{R(k)}	KP	WFD	T	TD
	(Ω)	(Ω)	(Ω/l)	s	s	s
1-2	112597	2798	-263517604	540	540	0
2-3	116317	2911	-272174404	780	240	540
3-4	117497	3110	-274528804	1200	420	780
4-5	117497	3617	-274192804	1620	420	1200
5-6	118078	5636	-269860804	2280	660	1620
6-7	117988	66222	-124238402	2580	300	2280
7-8	118048	115182	-6878400.11	-	-	-

Table 4_ARX1821 model parameters

Click here to download table: Table 4.doc

Table 4. Discrete Time ARX model: $A(z)\ y(t)=B(z)u(t)+C(z)e(t)$, sampling time, T=60 s. Step input= 4.1666666 l s^{-1}

ARX model parameter	Corresponding Measurement Electrode Set						
	1-2	2-3	3-4	4-5	5-6	6-7	7-8
a0	1.0000	1.0000	1.0000	1.0000	1.0000	1.0000	-
a1	-0.37897	-0.47339	-0.62963	-0.77049	-0.85439	-0.36124	-
a2	0.19443	0.70080	-0.65840	-2.03083	-0.22730	1.11668	-
a3	0.14272	-0.32766	-0.13960	0.88349	-0.68187	-1.13709	-
a4	-0.03729	0.18052	0.65926	2.14842	0.40903	0.06141	-
a5	0.21304	-0.12527	0.35733	0.06259	0.08157	0.52960	-
a6	-0.20419	-0.23919	-0.34367	-1.23370	0.81181	-3.11748	-
a7	-0.06286	0.15789	-0.17309	-0.53997	0.91995	-2.78393	-
a8	0.13831	-0.11519	-0.30188	-0.16207	0.10279	-1.42136	-
a9	0.18533	0.21532	0.39380	0.04104	1.03368	-1.54268	-
a10	-0.24367	-0.13053	0.29956	1.02644	-0.31035	-1.77034	-
a11	0.05505	0.37753	-0.14149	0.16264	-2.16421	-1.49676	-
a12	0.11645	-0.45462	-0.37456	-0.32231	-1.34513	-1.29485	-
a13	-0.11272	0.17880	-0.21478	-0.71859	-2.24715	-0.06898	-
a14	0.02651	-0.16823	0.566696	1.81381	-2.1502	-1.4206	-
a15	-0.11966	0.24215	0.04017	-1.51095	-1.12102	-0.90743	-
a16	0.13453	-0.32000	-0.15243	-2.00343	-1.89179	-1.44394	-
a17	-0.01555	0.25993	-0.12622	-0.07655	-2.31090	0.03786	-
a18	-0.02756	-0.07150	0.075217	3.19204	-0.22319	-2.07253	-
b0	0.0000	0.0000	0.0000	0.0000	0.00000	0.0000	-
b1	0.0000	0.0000	128289	267632166	-313529862	0.0000	-
b2	10058205	9745277	0.0000	0.0000	0.00000	-5061774185	-
c0	1.0000	1.0000	1.0000	1.0000	1.0000	1.0000	-
%FIT	98.53%	99.38%	98.36%	98.64%	99.02%	95.6%	-